



INDIAN INSTITUTE OF TECHNOLOGY, GANDHINAGAR

ME 207 FLUID DYNAMICS
[SPRING 2025]

**GROUP PROJECT
FLOW EVOLUTION IN WAKES**

By Group 3

Ada Sinha Aditi Singh Deepak Gadhav
23110011 23110014 23110110

Monisha Kavuri Kushagreek Basu
23110162 23110184

Under the supervision of:

**Prof. Dilip Srinivas Sundaram
Prof. Uddipta Ghosh
and
Prof. Vinod Narayanan**

23rd April 2025

1 Objectives

This experiment investigates the aerodynamic wake characteristics of a Formula 1 rear wing under different Drag Reduction System (DRS) configurations. The primary focus is on analyzing the evolution of wake flow patterns and visualizing the changes in the velocity profile with DRS activated (open) versus deactivated (closed). Detailed velocity measurements at various downstream positions were used to map and compare the wake structures in both configurations. Additionally, the experiment evaluates the impact of DRS on aerodynamic efficiency by calculating the drag coefficient (C_d) using the momentum deficit method. Before performing wind tunnel tests on the DRS setup, to verify the accuracy of our measurement technique and drag coefficient calculations, performing a similar analysis using a cylinder placed in the same wind tunnel section.

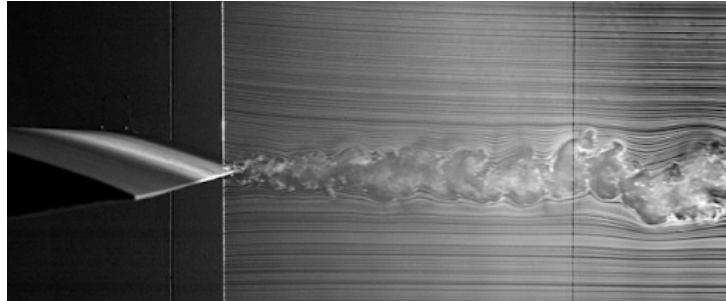


Figure 1: Wake visualization at the trailing edge of surfaces

2 Theoretical Discussions/Calculations

In Formula 1 aerodynamics, the rear wing plays a critical role in controlling drag and downforce. The Drag Reduction System (DRS) is a movable flap on the rear wing that can be opened to reduce drag and improve top speed on straights. Understanding the flow behavior in the wake of the rear wing and quantifying the drag under DRS ON and OFF conditions are essential for performance optimization. This section provides the theoretical basis for calculating the drag coefficient using wake measurements and introduces the momentum deficit method as the primary analytical tool.

The drag force on an airfoil (or any body) can be calculated by analyzing the velocity deficit in its wake. This derivation uses the principles of **conservation of mass** and **momentum** in fluid mechanics to derive the standard momentum deficit formula.

Assumptions

- **Steady, incompressible flow:** $\frac{\partial}{\partial t} = 0$, $\rho = \text{constant}$.
- **Inviscid flow outside the wake:** Pressure $P \approx P_\infty$ in the far field.
- **2D flow:** No variation in the spanwise (z) direction.
- **Thin wake:** Velocity deficit $U_\infty - u(y)$ is small compared to U_∞ .

Control Volume Analysis

Consider a control volume (CV) enclosing the airfoil:

- **Upstream (1):** Freestream velocity U_∞ , pressure P_∞ .
- **Downstream (2):** Wake velocity profile $u(y)$, pressure P_∞ (pressure recovery).

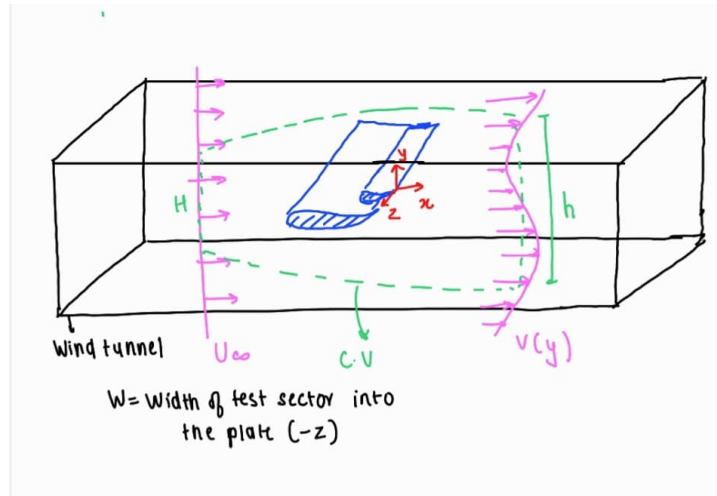


Figure 2: Control volume around the airfoil. The wake is measured downstream.

Conservation of Mass

For incompressible flow, mass flow rate must balance:

$$\int_{-\infty}^{\infty} U_\infty dy = \int_{-\infty}^{\infty} u(y) dy.$$

Due to the airfoil's presence, the wake has a **velocity deficit**:

$$\Delta u(y) = U_\infty - u(y).$$

Conservation of Momentum (x-Direction)

The drag force D equals the change in momentum flux across the CV:

$$D = \text{Momentum flux at (1)} - \text{Momentum flux at (2)}.$$

Expressed mathematically:

$$D = \rho \int_{-\infty}^{\infty} U_\infty^2 dy - \rho \int_{-\infty}^{\infty} u(y)^2 dy.$$

Using mass conservation, we subtract the mass flux deficit:

$$D = \rho \int_{-\infty}^{\infty} u(y) (U_\infty - u(y)) dy.$$

This is the **standard momentum deficit formula** for drag.

Simplification for Small Deficit

If $\Delta u \ll U_\infty$, we approximate:

$$D \approx \rho U_\infty \int_{-\infty}^{\infty} (U_\infty - u(y)) dy.$$

However, the exact form (used in computations) is:

$$D = \rho \int_{-\infty}^{\infty} u(y) (U_\infty - u(y)) dy.$$

Drag Coefficient

The drag coefficient C_D is normalized by dynamic pressure and reference area. For 2D airfoils:

$$C_D = \frac{2D}{\rho U_\infty^2 A},$$

where A is the Area of the test section. If using width W and height h , it becomes:

$$C_D = \frac{2D}{\rho U_\infty^2 Wh}.$$

Velocity Profile Comparison

- Lower velocity deficit in the wake indicates reduced drag (expected with DRS ON).
- A more streamlined wake implies less turbulence and improved flow reattachment.

Drag Coefficient

- Expected trend: $C_{D, \text{ON}} < C_{D, \text{OFF}}$.
- The drag coefficient (C_D) was computed using velocity profile data through trapezoidal integration of the momentum deficit.
- A custom code was developed to account for:
 - Freestream velocity,
 - Air density,
 - Wind tunnel width.

3 Experimental Setup

The experiment was conducted in a closed-loop subsonic wind tunnel with a test section width of 0.25 m. The test model consisted of two 3D-printed NACA 6409 airfoils: a main flap with a chord length of 150 mm and a DRS flap with a chord length of 60 mm. These were mounted using a custom acrylic fixture, designed with precision-cut holes to accommodate both DRS ON and DRS OFF configurations. The fixture also featured a stable base structure to minimize vibration during measurements.

The DRS mechanism operated in two distinct orientations:

- **DRS ON:** The DRS flap was aligned horizontally (0°).



Figure 3: Orientation of flaps when DRS is ON

- **DRS OFF:** The DRS flap was inclined at 30° with the horizontal.

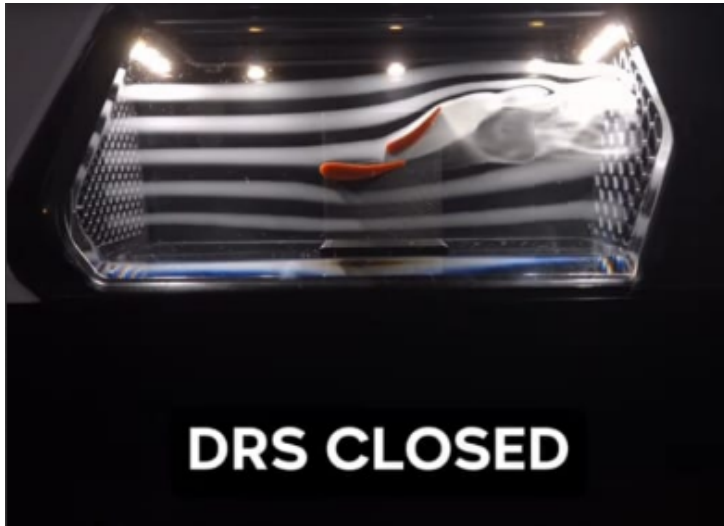


Figure 4: Orientation of flaps when DRS is OFF

The airfoils were fabricated using PLA via 3D printing. The mounting was done using a custom-designed rigid fixture with laser-cut acrylic sheets for structural stability and repeatable positioning.

Instrumentation and Measurement Techniques

To analyze the wake behavior and measure flow characteristics, the following tools and sensors were employed:

- **Pitot-Static Tube:** Used to sense flow velocity at each measurement point

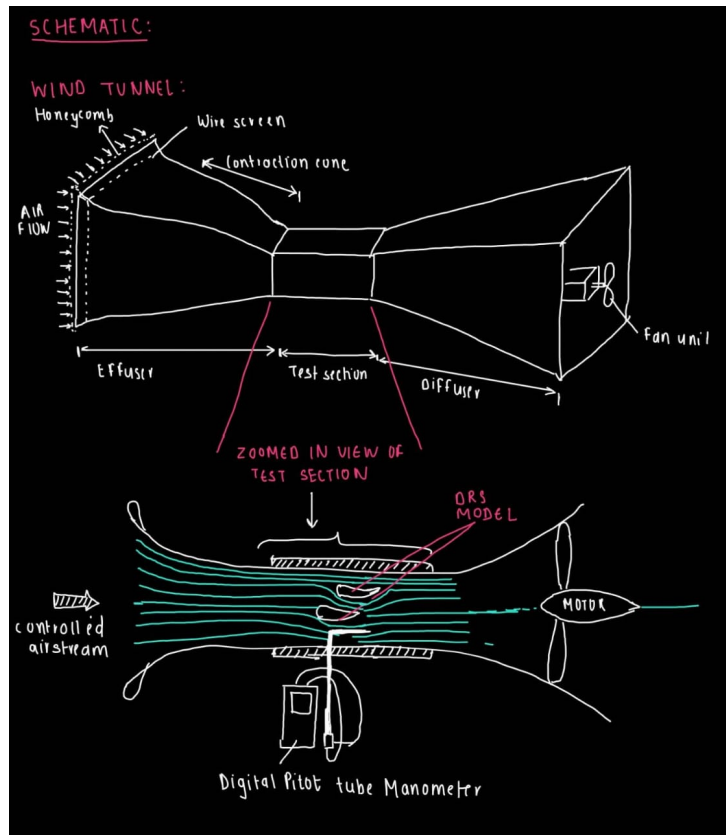


Figure 5: Schematic of the setup

- **Digital Micromanometer:** Directly displayed calibrated air velocity values, eliminating the need for manual Bernoulli-based conversions.
- **Vertical Traverse Mechanism:** The Pitot tube was vertically adjusted using a manual traverse system equipped with a **digital height gauge**, enabling precise placement at specific y-coordinates



Figure 6: Digital Height Gauge



Figure 7: Digital Micromanometer with Pitot Static Tube



Figure 8: DRS setup mounted in the test section



Figure 9: Pitot tube attached to digital height guage



Figure 10: DRS setup with the micro-manometer attached to the pitot tube



Figure 11: 3D-printed model mounted to the stand

This instrumentation allowed for high-resolution mapping of the wake profile, essential for computing the drag coefficient using the momentum deficit method.

Wake flow analysis was carried out using a Pitot-static tube connected to a digital micromanometer, which provided direct velocity readings at various downstream x- and vertical y-positions behind the rear wing. This setup was also used to determine the freestream velocity (u_∞) before data collection for each configuration.

4 Procedure

1. The wing model was securely mounted in the test section. The DRS flap was initially set to the DRS ON position (0° with the horizontal).
2. Freestream velocity $u_\infty = 6.2$ m/s was established and verified using upstream Pitot measurements without the model.
3. The Pitot tube was moved vertically along the y-axis at a fixed x-location downstream (ex: $x = 0$ mm). The tip of the DRS flap was set as $y = 0$ mm.
4. At each y-position, three velocity readings were recorded at 5 second intervals.
5. Measurements were repeated at various horizontal distances downstream ($x = 20, 40, 60, 80, 100,$ and 120 mm). These positions were marked on the test section with the help of a scale and the Pitot tube was manually adjusted to align with the markings.
6. Then the whole procedure was repeated for the DRS OFF condition as well.
7. Plots of y-values vs the average velocity were plotted for each of the horizontal distances.
8. Velocity profiles were input into a custom Python script that computed the drag force (F_D) via trapezoidal integration of the velocity deficit and subsequently derived the drag coefficient (C_D) using the momentum deficit method.
9. The test was performed at consistent flow conditions for accurate comparison.

The test was performed at consistent flow conditions for accurate comparison.

5 Validation study using a Cylindrical test body

To verify the accuracy of our measurement technique and drag coefficient calculations, a similar analysis was performed using a cylinder placed in the same wind tunnel setup. The cylinder is a well-studied benchmark in external flow aerodynamics, with widely accepted theoretical and experimental drag coefficient values available in literature.

By comparing our experimentally obtained drag coefficient for the cylinder with standard reference values, we validated the reliability of our methodology—including Pitot-based velocity profiling, data processing, and the momentum deficit approach for calculation of the coefficient of drag. This verification provided confidence in the accuracy

of our results and calculations applied to the more complex DRS configurations of the Formula 1 rear wing.

y (mm)	Reading 1 (m/s)	Reading 2 (m/s)	Reading 3 (m/s)	U_avg (m/s)
-25	1.33	1.29	1.25	1.29
-20	1.27	1.15	1.24	1.22
-15	1.31	1.03	1.20	1.18
-10	1.17	1.01	1.22	1.13
-5	1.11	0.91	1.17	1.06
0	1.07	0.81	1.21	1.03
5	1.09	0.87	1.25	1.07
10	1.13	0.89	1.34	1.12
15	1.29	1.01	1.24	1.18
20	1.37	1.03	1.20	1.20
25	1.39	1.09	1.21	1.23

Table 1: Velocity profile across the y-axis for cylindrical body

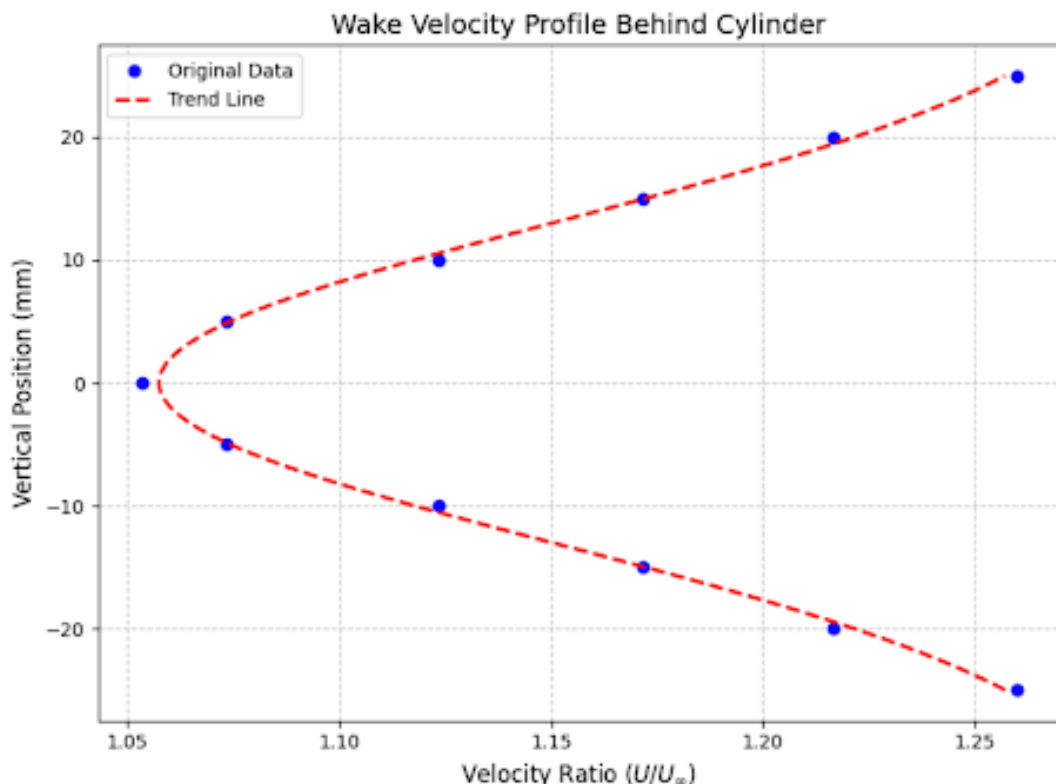


Figure 12: Wake velocity profile for cylinder

Calculation of coefficient of drag for cylinder:

A code snippet along with the output used for processing the cylinder wake data is included below to demonstrate the implementation and reproducibility of the analysis.

```

1 import numpy as np
2
3 # Wake velocity data at X = 0 mm

```

```

4 y_wake_mm = np.array([-25, -20, -15, -10, -5, 0, 5, 10, 15, 20,
5   25]) # in mm
6 u_wake = np.array([1.29, 1.22, 1.18, 1.13, 1.06,
7   1.03, 1.07, 1.12, 1.18, 1.20, 1.23]) # in m/s
8
9 # Convert Y positions to meters and sort both datasets
10 sorted_indices = np.argsort(y_wake_mm)
11 y = y_wake_mm[sorted_indices] * 1e-3 # in meters
12 u = u_wake[sorted_indices]
13
14 # Constants
15 rho = 1.225      # air density in kg/m^3
16 W = 0.25         # test section width in meters
17 D = 0.08         # diameter of cylinder in meters
18 u_inf = 1.5       # freestream velocity in m/s
19
20 # Reynolds number
21 Re = rho * u_inf * D / 1.81e-5
22
23 # Trapezoidal integration for Drag Force
24 FD = 0
25 for i in range(len(y) - 1):
26     dy = y[i+1] - y[i]
27     u_avg = (u[i] + u[i+1]) / 2
28     delta_u1 = (u_inf - u[i])
29     delta_u2 = (u_inf - u[i+1])
30     integrand_avg = (u_avg * (delta_u1 + delta_u2)) / 2
31     FD += integrand_avg * dy
32
33 FD *= rho
34
35 # Drag Coefficient
36 CD = (2 * FD) / (rho * (u_inf**2) * W * D)
37
38 # Results
39 print(f'L/D {W/D:.3f}')
40 print(f'Experimental Reynold's number: {Re}')
41 print(f'Experimental Freestream Velocity U_inf = {u_inf:.4f} m/s')
42 print(f'Drag Force FD = {FD:.4f} N')
43 print(f'Drag Coefficient CD = {CD:.4f}')
44 print("Theoretical CD value approximately 0.7 < CD < 0.8")

```

Console Output from Python Script

```

1 L/D 3.125
2 Experimental Reynold's number: 8121.546961325968
3 Experimental Freestream Velocity U_inf = 1.5000 m/s
4 Drag Force FD = 0.0246 N
5 Drag Coefficient CD = 0.8930
6 Theoretical CD value approximately 0.7 < CD < 0.8

```

The following results were obtained from the wake velocity measurements behind the cylindrical body using the same experimental procedure and data processing approach:

Freestream velocity = 1.5 m/s

Test section width = 0.25 m

Computed drag coefficient (C_D) = 0.893

The experimentally determined drag coefficient was compared with the standard reference value for a circular cylinder in subsonic flow conditions, typically between 0.7 and 0.8. The close agreement validates the effectiveness of the measurement technique and the momentum deficit method used throughout this study.

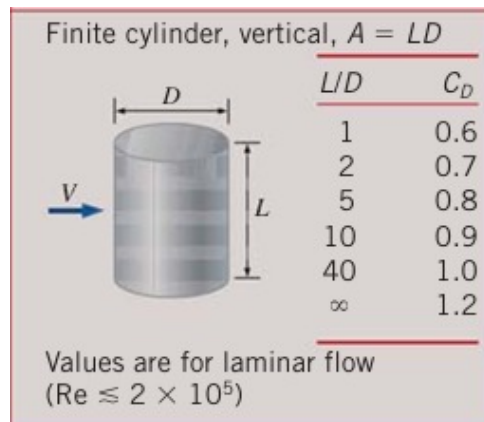


Figure 13: Finite cylinder drag coefficients (Source: Cengel, Cimbala)

Having established the reliability of the methodology through this benchmark test, the analysis now proceeds to the results obtained for the DRS configurations of the Formula 1 rear wing.

6 Experimental Observations & Analysis

A) Tabulated below are the obtained experimental values of the velocity profile along the wake at different **x locations** (downstream of the flow) with **DRS ON** Configuration:

i) $x = 0 \text{ mm}$

Table 2: Velocity profile data at $x = 0$ mm (DRS ON)

X = 0 mm				
Y (mm)	Reading 1 (m/s)	Reading 2 (m/s)	Reading 3 (m/s)	Avg velocity (m/s)
20	5.99	5.99	6.01	5.99
10	5.93	5.98	5.97	5.96
0	3.45	3.51	3.49	3.48
-10	4.88	4.88	4.92	4.89
-20	6.02	6.02	5.98	6.01
-30	6.15	6.15	6.10	6.13
-40	6.25	6.12	6.27	6.21
-50	6.17	6.13	6.04	6.11
-60	5.42	5.34	5.55	5.44

ii) $x = 20$ mm

Table 3: Velocity profile data at $x = 20$ mm (DRS ON)

X = 20 mm				
Y (mm)	Reading 1 (m/s)	Reading 2 (m/s)	Reading 3 (m/s)	Avg velocity (m/s)
20	5.96	6.03	5.98	5.99
10	5.90	5.91	5.89	5.90
0	4.54	4.54	4.47	4.52
-10	5.40	5.53	5.46	5.46
-20	6.03	6.03	6.10	6.05
-30	6.02	6.07	6.06	6.05
-40	5.91	5.81	6.04	5.92
-50	5.86	5.71	5.59	5.72
-60	5.04	5.16	5.04	5.08

iii) $x = 40$ mm

Table 4: Velocity profile data at $x = 40$ mm (DRS ON)

X = 40 mm				
Y (mm)	Reading 1 (m/s)	Reading 2 (m/s)	Reading 3 (m/s)	Avg velocity (m/s)
20	5.98	5.99	6.00	5.99
10	5.71	5.89	5.67	5.76
0	4.62	4.87	4.87	4.79
-10	5.77	5.65	5.81	5.74
-20	6.03	6.06	6.11	6.07
-30	5.85	5.99	5.90	5.91
-40	5.33	5.36	5.75	5.48
-50	4.99	4.92	4.94	4.95
-60	4.90	4.92	4.94	4.92

iv) $x = 60 \text{ mm}$

Table 5: Velocity profile data at $x = 60 \text{ mm}$ (DRS ON)

X = 60 mm				
Y (mm)	Reading 1 (m/s)	Reading 2 (m/s)	Reading 3 (m/s)	Avg velocity (m/s)
20	6.01	6.00	5.94	5.98
10	5.75	5.74	5.76	5.75
0	4.52	4.67	4.76	4.65
-10	5.81	5.91	5.82	5.85
-20	6.17	6.11	5.92	6.07
-30	5.87	6.06	5.81	5.91
-40	5.85	5.74	5.80	5.80
-50	5.33	5.24	5.25	5.27
-60	4.52	4.30	4.49	4.44

v) $x = 80 \text{ mm}$

Table 6: Velocity profile data at $x = 80 \text{ mm}$ (DRS ON)

X = 80 mm				
Y (mm)	Reading 1 (m/s)	Reading 2 (m/s)	Reading 3 (m/s)	Avg velocity (m/s)
20	5.98	5.96	5.93	5.96
10	4.98	4.92	4.95	4.95
0	5.01	5.17	5.06	5.08
-10	5.87	5.81	5.87	5.85
-20	6.02	6.01	5.99	6.01
-30	5.71	5.81	5.86	5.79
-40	5.67	5.74	5.14	5.52
-50	4.80	5.06	5.16	5.01
-60	3.87	4.24	4.15	4.09

vi) $x = 100 \text{ mm}$

Table 7: Velocity profile data at $x = 100 \text{ mm}$ (DRS ON)

X = 100 mm				
Y (mm)	Reading 1 (m/s)	Reading 2 (m/s)	Reading 3 (m/s)	Avg velocity (m/s)
20	5.74	5.71	5.75	5.73
10	4.27	4.86	4.83	4.65
0	5.23	5.21	5.20	5.21
-10	5.73	5.75	5.80	5.76
-20	5.96	6.01	5.87	5.95
-30	5.67	5.81	5.13	5.54
-40	4.56	4.51	4.37	4.48
-50	3.52	4.36	4.31	4.06
-60	3.52	4.36	3.37	3.75

viI) $x = 120$ mm

Table 8: Velocity profile data at $x = 120$ mm (DRS ON)

X = 120 mm				
Y (mm)	Reading 1 (m/s)	Reading 2 (m/s)	Reading 3 (m/s)	Avg velocity (m/s)
20	5.64	5.64	5.62	5.63
10	4.95	4.96	4.92	4.94
0	5.28	5.33	5.26	5.29
-10	5.63	5.71	5.61	5.65
-20	5.70	5.74	5.78	5.74
-30	5.48	5.39	5.53	5.47
-40	4.98	4.84	5.05	4.96
-50	4.10	4.29	4.76	4.38
-60	3.41	3.41	3.64	3.49

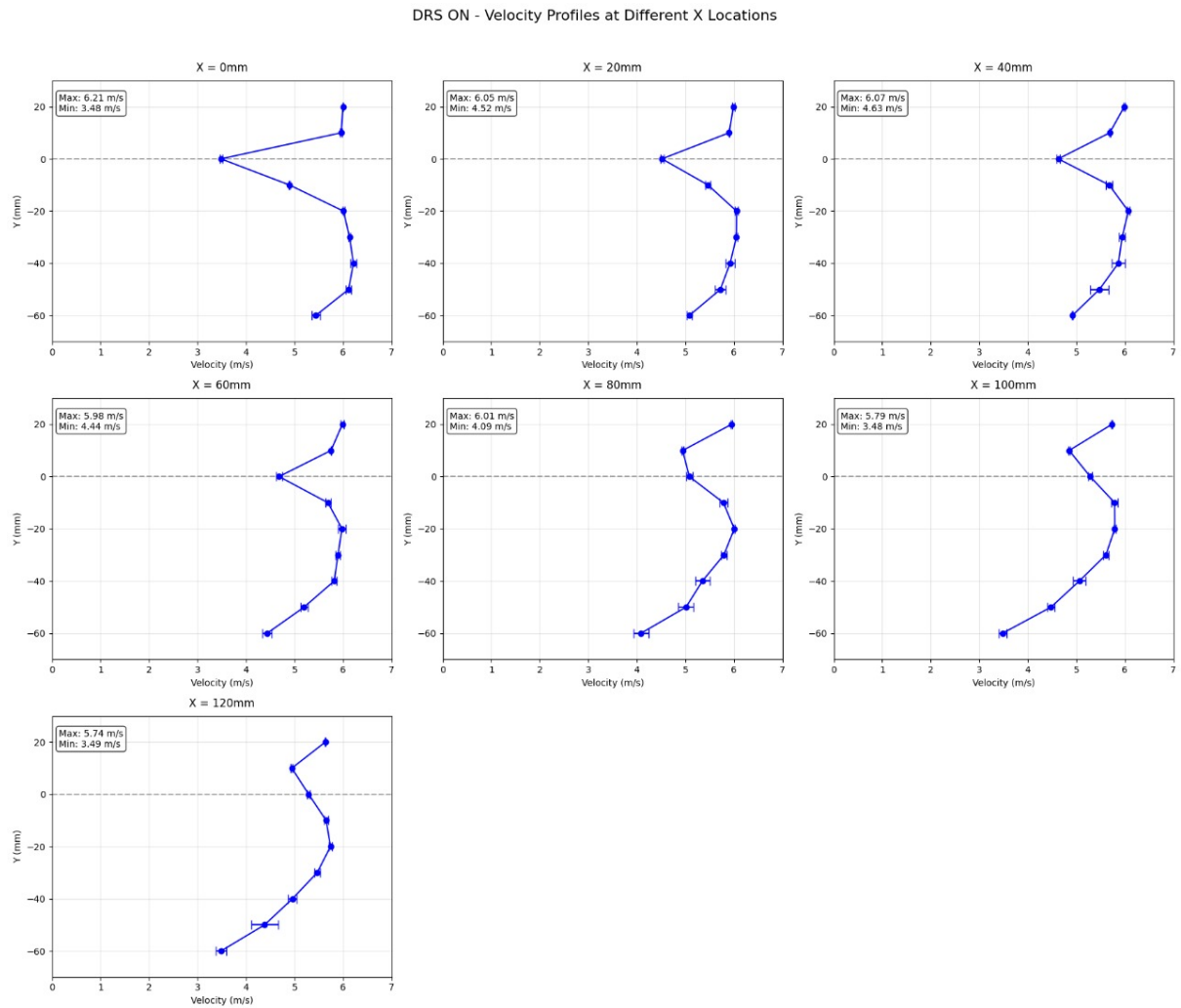


Figure 14: Visualization of velocity profile across various x location with DRS ON configuration

B) Tabulated below are the obtained experimental values of the velocity profile along the wake at different **x locations** (downstream of the flow) with **DRS OFF** Configuration:

i) $x = 0 \text{ mm}$

Table 9: Velocity profile data at $x = 0 \text{ mm}$ (DRS OFF)

X = 0 mm				
Y (mm)	Reading 1 (m/s)	Reading 2 (m/s)	Reading 3 (m/s)	Avg velocity (m/s)
20	6.63	5.82	5.63	6.03
10	5.33	5.45	4.94	5.24
0	4.07	3.94	3.35	3.79
-10	3.66	3.64	3.41	3.57
-20	3.83	3.88	3.48	3.73
-30	6.18	6.21	6.10	6.16
-40	6.02	6.05	6.01	6.03
-50	5.81	5.80	5.90	5.84
-60	6.81	5.80	5.90	5.98

ii) $x = 20 \text{ mm}$

Table 10: Velocity profile data at $x = 20 \text{ mm}$ (DRS OFF)

X = 20 mm				
Y (mm)	Reading 1 (m/s)	Reading 2 (m/s)	Reading 3 (m/s)	Avg velocity (m/s)
20	6.77	5.92	5.85	6.18
10	6.04	3.56	3.55	4.38
0	4.07	3.94	3.86	3.96
-10	1.92	1.58	1.06	1.52
-20	5.87	5.86	5.71	5.81
-30	6.01	5.98	5.70	5.90
-40	6.06	5.88	5.60	5.85
-50	6.06	5.88	5.90	5.95
-60	5.86	5.84	5.90	5.87

iii) $x = 40 \text{ mm}$

Table 11: Velocity profile data at $x = 40$ mm (DRS OFF)

X = 40 mm				
Y (mm)	Reading 1 (m/s)	Reading 2 (m/s)	Reading 3 (m/s)	Avg velocity (m/s)
20	2.85	5.79	5.70	4.78
10	2.50	2.50	2.50	2.50
0	2.25	2.25	2.25	2.25
-10	2.20	2.37	2.03	2.20
-20	4.64	4.40	4.60	4.55
-30	5.87	5.76	5.64	5.76
-40	5.80	5.68	5.75	5.74
-50	5.54	5.58	5.61	5.58
-60	5.22	5.02	4.96	5.07

iv) $x = 60$ mm

Table 12: Velocity profile data at $x = 60$ mm (DRS OFF)

X = 60 mm				
Y (mm)	Reading 1 (m/s)	Reading 2 (m/s)	Reading 3 (m/s)	Avg velocity (m/s)
20	4.59	4.52	4.48	4.53
10	4.16	4.18	4.13	4.16
0	4.77	4.84	4.98	4.86
-10	5.66	5.64	5.72	5.67
-20	5.80	5.82	5.84	5.82
-30	5.78	5.61	5.69	5.69
-40	5.33	5.72	5.75	5.60
-50	4.79	4.72	4.45	4.65
-60	4.55	4.15	4.19	4.30

v) $x = 80$ mm

Table 13: Velocity profile data at $x = 80$ mm (DRS OFF)

X = 80 mm				
Y (mm)	Reading 1 (m/s)	Reading 2 (m/s)	Reading 3 (m/s)	Avg velocity (m/s)
20	4.71	4.64	4.52	4.62
10	4.67	4.91	4.76	4.78
0	5.51	5.43	5.45	5.46
-10	5.80	5.74	5.91	5.82
-20	5.73	5.81	5.92	5.82
-30	5.49	5.74	5.62	5.62
-40	4.78	4.88	5.12	4.93
-50	4.28	4.34	4.29	4.30
-60	3.46	3.38	4.00	3.61

vi) $x = 100 \text{ mm}$

Table 14: Velocity profile data at $x = 100 \text{ mm}$ (DRS OFF)

X = 100 mm				
Y (mm)	Reading 1 (m/s)	Reading 2 (m/s)	Reading 3 (m/s)	Avg velocity (m/s)
20	4.69	4.85	4.72	4.75
10	5.31	5.27	5.27	5.28
0	5.77	5.59	5.64	5.67
-10	5.74	5.74	5.71	5.73
-20	5.88	5.72	5.56	5.72
-30	5.22	5.07	5.20	5.16
-40	4.85	4.74	4.43	4.67
-50	4.05	3.62	3.76	3.81
-60	2.70	2.91	2.81	2.81

vii) $x = 120 \text{ mm}$

Table 15: Velocity profile data at $x = 120 \text{ mm}$ (DRS OFF)

X = 120 mm				
Y (mm)	Reading 1 (m/s)	Reading 2 (m/s)	Reading 3 (m/s)	Avg velocity (m/s)
20	5.04	5.14	5.06	5.08
10	5.48	5.45	5.30	5.41
0	5.73	5.71	5.70	5.71
-10	5.64	5.60	5.82	5.69
-20	5.33	5.41	5.50	5.41
-30	5.00	5.09	4.65	4.91
-40	3.80	4.25	4.14	4.06
-50	3.63	3.19	3.43	3.42
-60	2.83	2.84	2.91	2.86

DRS OFF - Velocity Profiles at Different X Locations

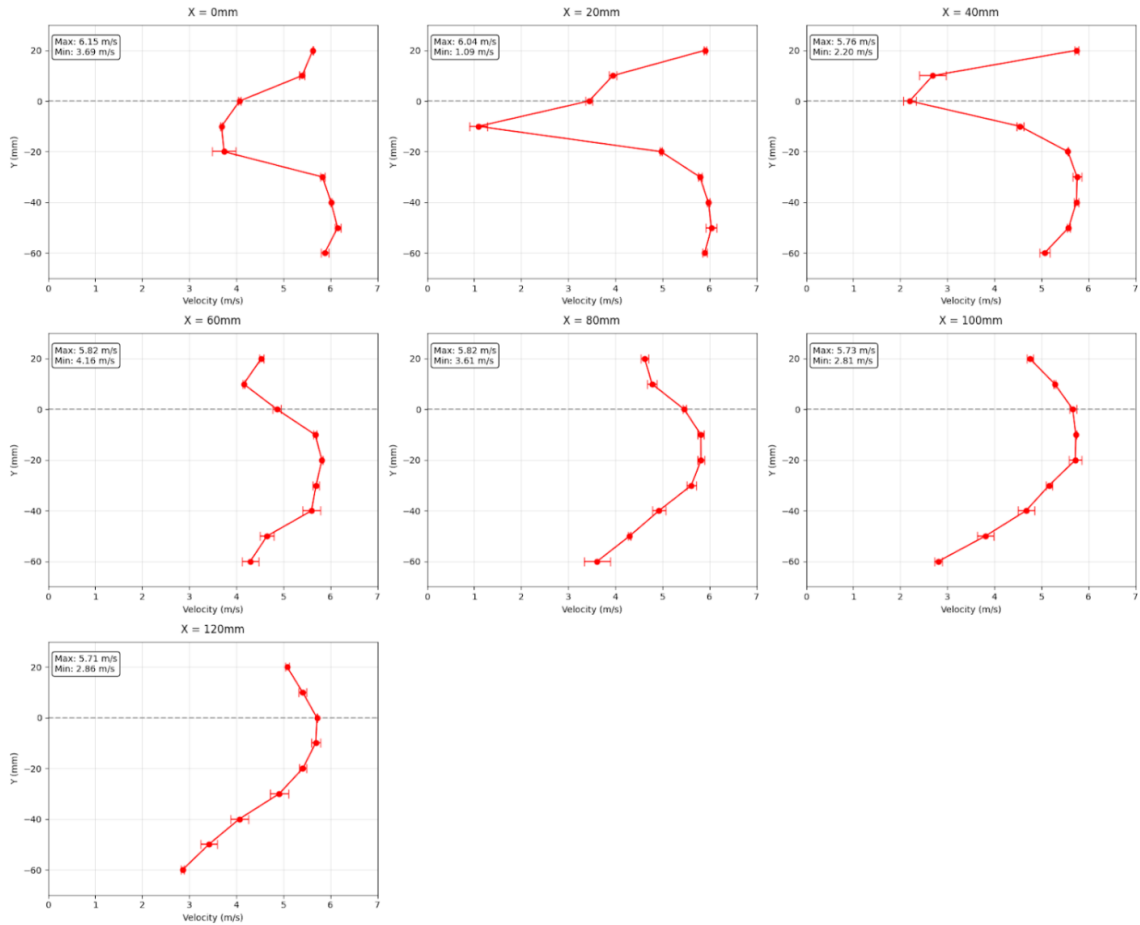


Figure 15: Visualization of velocity profile across various x location with DRS OFF configuration

C) The following code is implemented to calculate drag coefficient and drag force on the airfoil at various x values:

```

1 import numpy as np
2
3 # Wake velocity data at X = 0 mm
4 y_wake_mm = np.array([20, 10, 0, -10, -20, -30, -40, -50, -60])
5 # in mm
6
7 u_wake = np.array([5.9967, 5.96, 5.4833, 4.8933, 6.0067, 6.1333,
8 6.2133,
9 6.1133, 5.4367]) # in m/s
10
11 # Convert Y positions to meters and sort both datasets
12 sorted_indices = np.argsort(y_wake_mm)
13 y = y_wake_mm[sorted_indices] * 1e-3 # in meters
14 u = u_wake[sorted_indices]
15
16 # Constants
17 rho = 1.225 # air density in kg/m^3

```

```

16 W = 0.25           # test section width in meters
17 h = 0.1            # test height width in meters (-20 to 60)
18 u_inf = 6.2        # freestream velocity in m/s
19
20 # Trapezoidal integration for Drag Force
21 FD = 0
22 for i in range(len(y) - 1):
23     dy = y[i+1] - y[i]
24     u_avg = (u[i] + u[i+1]) / 2
25     delta_u1 = (u_inf - u[i])
26     delta_u2 = (u_inf - u[i+1])
27     integrand_avg = (u_avg * (delta_u1 + delta_u2)) / 2
28     FD += integrand_avg * dy
29
30 FD *= rho
31
32 # Drag Coefficient
33 CD = (2 * FD) / (rho * (u_inf**2) * W * h)
34
35 # Results
36 print(f"Experimental Freestream Velocity U_inf = {u_inf:.4f} m/s")
37 print(f"Drag Force FD = {FD:.4f} N")
38 print(f"Drag Coefficient CD = {CD:.4f}")

```

This code inputs the average velocity readings across varying y-directions at a fixed x-point ($X = 0$ mm) behind an object in a flow field. It processes the vertical positions (y_{wake_mm}) and corresponding velocity measurements (u_{wake}), converting them to meters and sorting them for analysis.

Using the freestream velocity ($u_\infty = 6.2$ m/s), it calculates the drag force (FD) by integrating the velocity deficit across the wake profile via trapezoidal integration, accounting for air density ($\rho = 1.225$ kg/m³) and test section width ($W = 0.25$ m). Finally, it computes the drag coefficient (CD) and prints the results.

D) Tabulated below are the calculated Drag coefficient values at every x position for **DRS ON** configuration and **DRS OFF** configuration:

Table 16: Calculated drag coefficient C_d at various x positions for DRS ON and DRS OFF configurations

x (mm)	C_d (DRS ON)	C_d (DRS OFF)
0	0.5089	0.8158
20	0.4990	0.8910
40	0.5380	0.9624
60	0.5949	0.8761
80	0.7094	0.8696
100	0.8253	0.9112
120	0.8696	0.9753

7 Results & Discussions

A) Comparison of Experimental and CFD Results for DRS OFF Configuration

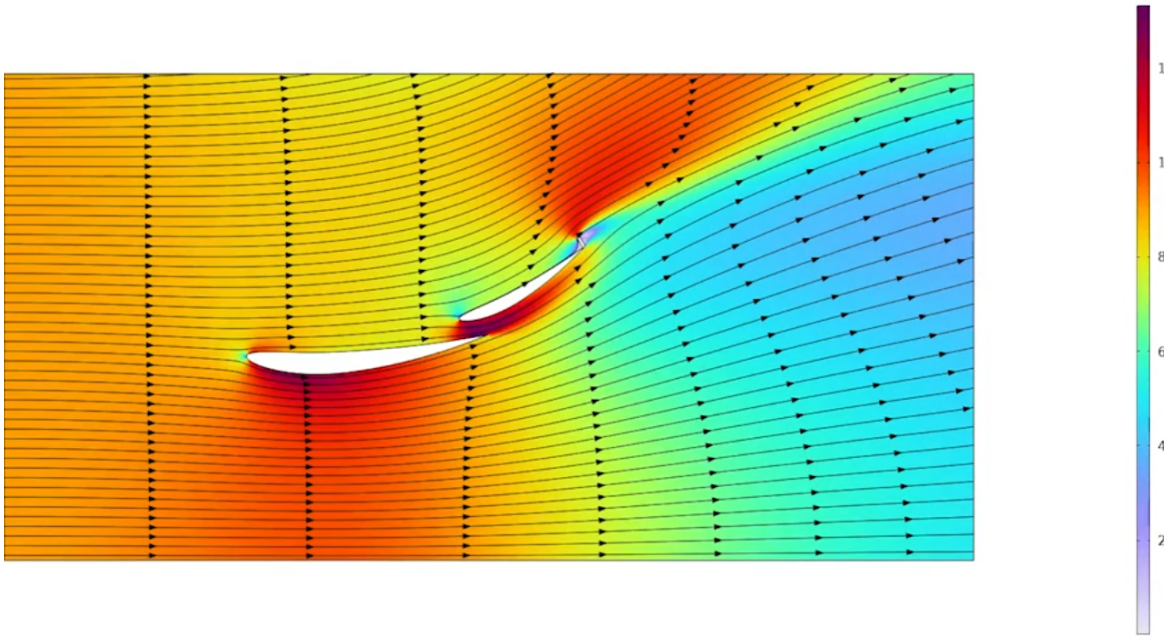


Figure 16: Source: “*Modeling Drag Reduction Systems for Motorsports Using CFD*,” COMSOL, 2024.

<https://www.comsol.com/blogs/modeling-drag-reduction-systems-for-motorsports-using-cfd>

The experimental velocity profiles demonstrate a high degree of agreement with the CFD simulation in terms of wake location, minimum velocity values and flow recovery. While the velocity magnitudes differ due to scale, the trends and velocity profile observed experimentally accurately reflect the *behavior* predicted by the COMSOL simulation, validating the experimental setup and suggesting that the wind tunnel and probe measurements are effective for DRS configurations.

1. Wake Formation and Minimum Velocity Comparison

The CFD velocity contour illustrates a prominent wake region with significantly reduced velocity behind the trailing edge of the DRS flap wing. This is supported by our experimental data, where the velocity profiles at **x = 20 mm** show a drop to a **minimum of 1.09 m/s**. This low value highlights the immediate flow separation and energy loss in the wake zone, which aligns with the dark blue region visible in the CFD plot.

As the flow moves downstream:

- At **X = 40 mm**, the minimum velocity increases to **2.20 m/s**.

- At **X = 60 mm**, it further rises to **4.16 m/s**.
- By **X = 100 mm** and **X = 120 mm**, the minimum velocity reaches around **2.81 m/s** and **2.86 m/s**, respectively.

2. Maximum Velocity Comparison and Profile Shape

The CFD simulation indicates a freestream velocity approaching ~ 100 m/s, representing the maximum domain value. In contrast, the experimental values are naturally scaled down due to wind tunnel and model constraints, with maximum measured velocities across sections ranging from:

- **6.15 m/s at X = 0 mm**
- **5.71 m/s at X = 120 mm**

Despite the difference in magnitude, the **shape** of the profiles is consistent with the CFD analysis. Each profile exhibits a high velocity in the outer flow region and a central dip in the wake, suggesting that the experimental setup captures the shear layer structure and core wake dynamics.

3. Wake Width and Symmetry Analysis

The CFD contours reveal a moderately wide wake that slowly narrows and stabilizes as the flow recovers. This is well reflected in the experimental plots. For instance:

- At **X = 20 mm**, the wake spans almost the entire vertical measurement range ($Y = \pm 60$ mm), showing asymmetry and turbulent mixing.
- At **X = 80–120 mm**, the wake shape becomes more uniform and symmetric, with less variation across the Y-axis and smoother profile curvature.

The transition from asymmetric, sharp profiles to smoother and more stable ones also indicates that **turbulent diffusion and reattachment are correctly captured** in both simulation and experiment.

B) Comparison of Experimental and CFD Results for DRS ON Configuration

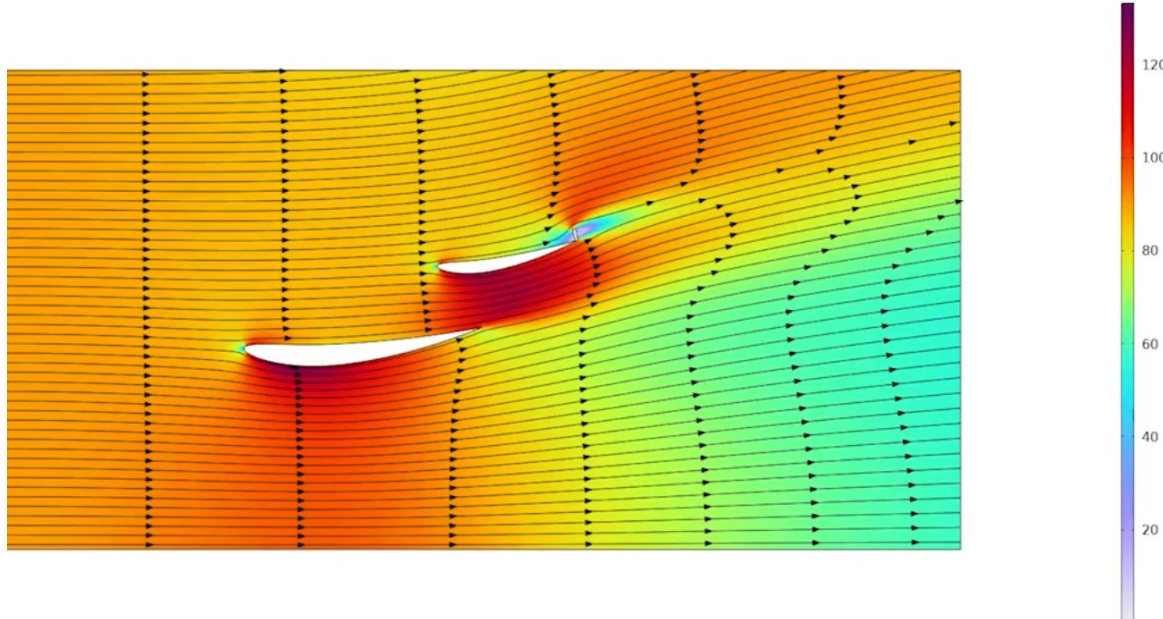


Figure 17: Source: “*Modeling Drag Reduction Systems for Motorsports Using CFD*,” COMSOL, 2024.
<https://www.comsol.com/blogs/modeling-drag-reduction-systems-for-motorsports-using-cfd>

1. Overall Flow Characteristics from CFD:

The CFD velocity contour for the DRS ON configuration exhibits a clear reduction in wake intensity behind the rear wing. The airflow remains more attached, and the wake appears narrower compared to the DRS OFF case, which is consistent with the function of the Drag Reduction System (DRS) ON configuration that opens a slot gap between the main flap and the DRS flap to reduce drag. Velocity contours indicate high flow speed in the freestream, while wake regions show diminished flow speeds due to vortex shedding and pressure losses.

2. Experimental Velocity Profiles:

The experimental velocity profiles measured at different X-locations (from $X = 0$ mm to $X = 120$ mm) support the CFD insights:

- **$X = 0$ mm to $X = 40$ mm:** The maximum average velocity remains in the range of **5.9–6.3 m/s**, with the lowest observed value around **4.5 m/s**, suggesting limited wake effect immediately downstream. The velocity gradient near the centerline is smooth, confirming low obstruction and drag in this region.

- **X = 60 mm to X = 100 mm:** A symmetric double-peak shape is visible in most plots, indicating split flow paths due to the open DRS flap. Maximum velocities stay close to **6.2 m/s**, while minimum velocity stays between **3.9–4.5 m/s**, showing slight but controlled wake growth.
- **X = 120 mm:** The velocity continues to recover showcasing better symmetry **while values remain high**, indicating efficient wake management due to the DRS-induced flow **reattachment** and reduced pressure drag.

3. Accuracy and Similarity to CFD:

There is **strong agreement** between the CFD contour and the experimental profile patterns:

- The **shape of velocity profiles** matches the narrowing and steady recovery of the wake observed in the simulation.
- **Peak velocity values** are consistent (5.9–6.3 m/s), suggesting good experimental fidelity.
- The **minimum velocities** in wake regions (~ 3.9 m/s) also align well with the low-speed zones in the CFD.

Minor deviations are natural due to experimental turbulence, probe resolution limits, or 3D flow effects not fully captured in a 2D profile. However, overall accuracy is high, and the experimental data validates the simulated DRS ON effect effectively.

C) Comparison of Calculated Drag Coefficients in DRS ON vs DRS OFF

X (mm)	Cd (DRS ON)	Cd (DRS OFF)	% Reduction in Cd	Interpretation
0	0.5089	0.8158	37.25%	Substantial drag reduction is observed right at the start of the measurement zone reflecting the immediate impact of DRS, which promotes flow attachment and reduces pressure drag as soon as the air flow passes the wing.
20	0.4990	0.8910	44.64%	The maximum drag reduction occurs in this region, indicating this is likely the region where wake separation is strongest without DRS, and DRS most effectively mitigates it.
40	0.5380	0.9624	43.97%	Still in the high-impact zone of DRS. Even as the wake starts to evolve, the benefits from the DRS remain significant, maintaining drag reduction above 40%.
60	0.5949	0.8761	32.40%	The flow begins to partially recover, but DRS continues to offer a notable drag advantage, albeit at a comparatively decreasing rate.
80	0.7094	0.8696	17.89%	Reduction begins to diminish quite sharply in this region, suggesting reduced sensitivity to DRS in this mid-wake region, where turbulence and mixing dominate.
100	0.8253	0.9112	9.51%	The flow is in a late wake state, with limited influence from the upstream DRS configuration. Drag reduction is minor, but still present.
120	0.8696	0.9753	10.90%	Slight increase in Cd for both cases; the drag gap narrows, highlighting that the DRS effect has mostly dissipated downstream.

Table 17: Comparison of drag coefficients (Cd) at various X-locations for DRS ON and DRS OFF configurations.

INTERPRETATION OF RESULTS

DRS is most impactful in the initial wake development phase, where it significantly delays flow separation and reduces pressure drag. However, its effectiveness diminishes as the wake becomes more turbulent and mixed downstream. This suggests that DRS is optimally beneficial in short-track aerodynamic applications (e.g., Formula 1 straights) where immediate drag reduction translates to higher straight-line speeds, while its long-distance influence is limited. Final Verdict: DRS is a highly effective drag-reduction tool in the near-wake region but has reduced utility in fully developed turbulent wake flows. Its strategic deployment should focus on zones where early flow attachment provides the greatest performance advantage.

8 Conclusion

This study successfully demonstrated the aerodynamic impact of the Drag Reduction System (DRS) on the wake flow behind a Formula 1 rear wing. Experimental measurements confirmed that activating the DRS significantly reduces wake velocity deficits and drag coefficients, especially in the near-wake region (up to 60 mm downstream). The calculated drag coefficients showed a consistent reduction of up to 45% with DRS ON, validating its effectiveness in minimizing pressure drag and enhancing aerodynamic efficiency. These findings were strongly corroborated by CFD simulations performed by COMSOL, affirming the reliability of the experimental methodology and the strategic utility of DRS in high-speed racing applications.

9 Acknowledgements

We want to express our gratitude to Prof. Dilip Srinivas Sundaram, Prof. Udipta Ghosh, Prof Vinod Narayanan and TA's for their valuable guidance and assistance during this course. We are also thankful to the machine shop staff for providing us with the instruments. Their expertise and support were instrumental in the successful completion of the project. Thank you for sharing your knowledge and contributing to our learning experience.

References

- [1] COMSOL, “Modeling Drag Reduction Systems for Motorsports Using CFD,” [Online]. Available: <https://www.comsol.com/blogs/modeling-drag-reduction-systems-for-motorsports-using-cfd>. [Accessed: Apr. 23, 2025].
- [2] P. J. Pritchard, *Fox and McDonald’s Introduction to Fluid Mechanics*, 8th ed., 2011.
- [3] Y. A. Cengel and J. M. Cimbala, *Fluid Mechanics*, 2nd ed., 2004.
- [4] [Online]. Available: <https://engineering.purdue.edu/aae520/kay-chibana-wake-rpt.pdf>. [Accessed: Apr. 23, 2025].